Efficient production of [*n*]rotaxanes by using template-directed clipping reactions

Jishan Wu*, Ken Cham-Fai Leung†, and J. Fraser Stoddart‡

California NanoSystems Institute and Department of Chemistry and Biochemistry, University of California, 405 Hilgard Avenue, Los Angeles, CA 90095

Edited by Ronald Breslow, Columbia University, New York, NY, and approved August 27, 2007 (received for review June 21, 2007)

In this article, we report on the efficient synthesis of well defined, homogeneous [*n*]rotaxanes (*n* up to 11) by a template-directed thermodynamic clipping approach. By employing dynamic covalent chemistry in the form of reversible imine bond formation, [*n*]rotaxanes with dialkylammonium ion (–$CH_2NH_2^+CH_2$–) recognition sites, encircled by [24]crown-8 rings, were prepared by a thermodynamically controlled, template-directed clipping procedure, that is, by mixing together a dumbbell compound containing a discrete number of –$CH_2NH_2^+CH_2$– ion centers with appropriate amounts of a dialdehyde and a diamine to facilitate the [*n*]rotaxane formation. A 21-component self-assembly process is operative during the formation of the [11]rotaxane. The oligomeric dumbbells containing –$CH_2NH_2^+CH_2$– ion recognition sites were prepared by a stepwise protocol. Several of the dynamic [*n*]rotaxanes were converted into their kinetically stable counterparts, first by reduction (''fixing'') of imine bonds with the BH_3·THF complex, then by protonation of the complex by addition of acid.

dynamic covalent chemistry | molecular recognition | polyrotaxanes | self-assembly | template-directed synthesis

Mechanically interlocked and knotted compounds, such as rotaxanes (1–5), catenanes (6–10), suitanes (11, 12), trefoil knots (13–17), Borromean rings (18–20), and Solomon knots (21), represent challenging synthetic goals that have nevertheless been realized. These molecular compounds are usually synthesized by a template-directed approach (22) that depends on molecular recognition and self-assembly processes. Recently, their potential applications as molecular switches for nanoelectronics (23, 24) and molecular actuators for constructing artificial muscles (25), for fabricating smart surface materials (26), and for controlling the nanoscale release of molecules trapped in mesoporous silica (27–29) were demonstrated. Polyrotaxanes and well defined, homogeneous oligorotaxanes, in which the recognition sites on a dumbbell (an axle terminated by bulky stoppers) are encircled by large rings or macrocycles (wheels) by dint of molecular recognition, have become (30–36) one of the most intensively investigated subjects in mechanical chemistry. A general synthetic method for making rotaxanes, namely, the ''threading-followed-by-stoppering'' approach (Fig. 1, method A), involves (30–32) several macrocycles. First, the macrocycles are threaded onto oligomeric or polymeric axles carrying recognition sites at prescribed intervals along the axles to form pseudorotaxanes, then both ends of the axles are stoppered with bulky groups. Although this approach is relatively simple, it does not provide complete control over the number of threaded macrocycles, that is, the rings or beads are often not threaded onto all of the available recognition sites on the axles. Alternatively, a template-directed ''clipping'' approach (Fig. 1, method B), in which the macrocycles are formed from acyclic precursors in the presence of templating recognition sites on the dumbbells, has provided (33–36) a versatile means for the construction of some lower-order rotaxanes. Nonetheless, the efficient synthesis of well defined, homogeneous, higher-order polyrotaxanes continues to be a challenge to synthetic chemists.

Recently, dynamic covalent chemistry (37–40), exemplified by reversible imine formation (41, 42), metal–ligand exchange (43), and olefin metathesis (44, 45), has been demonstrated to be an effective tool for the preparation of various exotic mechanically interlocked molecular compounds. It has been found that, in the presence of an appropriate template, one of the possible compounds in the dynamic library, after mixing the different components, can be amplified to give the thermodynamically most stable product. We have reported (see refs. 46–49) an example of such a template-directed synthesis of linear and branched [*n*]rotaxanes ($n = 2$–4) by employing dynamic covalent chemistry in the form of reversible imine formation (Fig. 2*A*). In the presence of the dumbbell-shaped compound **1-H**·PF_6 containing a –$CH_2NH_2^+CH_2$– ion recognition site, the condensation of 2,6-pyridinedicarboxaldehyde (**2a**) and tetraethyleneglycol bis(2-aminophenyl)ether (**3**) forms selectively and near quantitatively a [24]crown-8 ring that becomes clipped onto the dumbbell. Such thermodynamically controlled, template-directed amplification is driven by a series of noncovalent bonding interactions that include [N^+–H···X] (X = O or N) and [N^+C–H···O] hydrogen bonds and aromatic π–π interactions between the dumbbell and the ring. The thermodynamic product, a [2]rotaxane, was converted into a stable [2]rotaxane by reduction (''fixing'') of the two imine bonds. Moreover, such a template-directed, thermodynamic clipping approach has proven (48, 49) to be effective and efficient in the synthesis of sterically bulky, mechanically interlocked dendrimers. Inspired by the success of this thermodynamically controlled approach, we became inter-

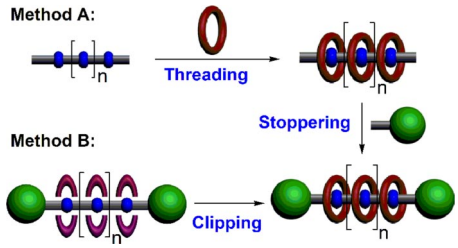

Fig. 1. Conceptual approaches to the template-directed syntheses of polyrotaxanes by using different protocols. (*Method A*) The ''threading-followed-by-stoppering'' approach. (*Method B*) The thermodynamically controlled clipping approach.

Author contributions: J.W. and J.F.S. designed research; J.W. performed research; K.C.-F.L. contributed new reagents/analytic tools; J.W. and J.F.S. analyzed data; and J.W., K.C.-F.L., and J.F.S. wrote the paper.

The authors declare no conflict of interest.

This article is a PNAS Direct Submission.

Abbreviations: TFA, trifluoroacetic acid; Boc, *tert*-butoxycarbonyl; PCC, pyridinium chlorochromate; HR-ESI-MS, high-resolution electrospray ionization mass spectra.

*Present address: Department of Chemistry, National University of Singapore, 3 Science Drive 3, Singapore 117543.

†Present address: Department of Chemistry, Chinese University of Hong Kong, Shatin, NT, Hong Kong Special Administrative Region, People's Republic of China.

‡To whom correspondence should be addressed at: Department of Chemistry and Biochemistry, University of California, 405 Hilgard Avenue, Los Angeles, CA 90095. E-mail: stoddart@chem.ucla.edu.

This article contains supporting information online at www.pnas.org/cgi/content/full/0705847104/DC1.

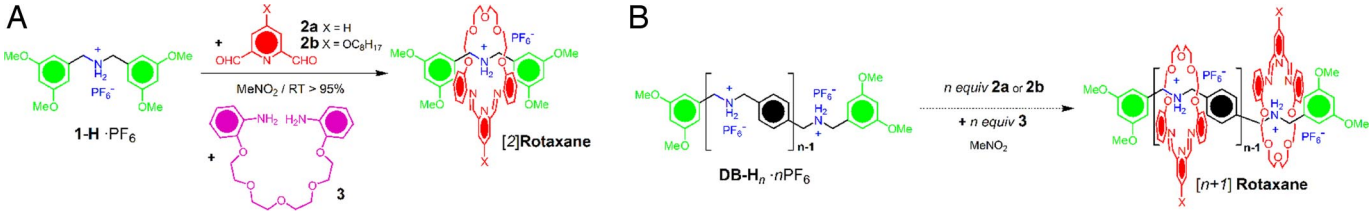

Fig. 2. Extrapolating from the past to the future in the synthesis of rotaxanes. (*A*) An example of the template-directed synthesis of a [2]rotaxane by using a clipping reaction. (*B*) The proposed template-directed synthesis of [n + 1]rotaxanes by employing clipping reactions on the dumbbells **DB-H$_n$**·nPF$_6$ as templates.

ested in synthesizing well defined, homogeneous, oligo- and polyrotaxanes under template control. In particular, we questioned whether mixing well defined homogeneous, dumbbell compounds **DB-H$_n$**·nPF$_6$ that already contain a known number of n –$CH_2NH_2^+CH_2$– ion recognition sites, together with n equivalents of the dialdehyde **2a** (or its alkoxy derivative **2b**) and n equivalents of the diamine **3**, would afford (Fig. 2*B*) an [n + 1]rotaxane in a one-pot, multicomponent self-assembly process. This process is much more challenging than the synthesis of randomly threaded polyrotaxanes for the following reasons: (*i*) it requires the synthesis of dumbbell-shaped templates with a well defined number of ion centers; (*ii*) subsequently, the formation of the [n]rotaxanes relies on successful and efficient template-directed condensations of (2n − 1) components [one dumbbell plus (n − 1) **2a** or **2b** plus (n − 1) **3** in one pot]; and (*iii*) the fixing of the dynamic [n]rotaxanes to give kinetically stable [n]rotaxanes after reduction of (2n − 2) imine bonds in a one-step, one-pot reaction. Herein, we report a detailed investigation of the efficient syntheses of well defined, homogeneous, higher-order oligo- and polyrotaxanes, employing the template-directed, thermodynamically controlled clipping approach (Fig. 1, method B).

Results and Discussion

The stepwise synthesis of the oligomeric dumbbell templates **DB-H$_n$**·nPF$_6$ is summarized in Fig. 3. The –$CH_2NH_2^+CH_2$– ion recognition centers were generated first by reductive amination with derivatives of benzylamines and benzaldehydes, then by protonation of the secondary amines and counterion exchange. In the synthesis of **DB-H$_n$**·nPF$_6$, 1 eq of *p*-xylenediamine (**4**) and 2 eq of the monoformyl-terminated half dumbbells **MA-*m*** (m = 0, 1, 2, 4, and 6), which contain a well defined number of *tert*-butoxycarbonyl (Boc)-protected dialkylamine functions, were condensed, affording the corresponding imines. In particular, the 3,5-dimethoxybenzyl groups serve as bulky stoppers to prevent the dethreading of rings from the axles of dumbbell components of the rotaxanes. Subsequently, the imine functions obtained after condensation were converted quantitatively into dialkylamino groups in **5(*m*)** by reduction with $NaBH_4$. Treatment of **5(*m*)** with trifluoroacetic acid (TFA) resulted in the quantitative removal of all of the Boc protecting groups to afford the **DB-H$_n$**·nTFA derivatives. After counterion exchange with saturated aqueous NH_4PF_6 solution, the corresponding dumbbell compounds **DB-H$_n$**·nPF$_6$ containing –$CH_2NH_2^+CH_2$– ion recognition sites were obtained in high yield. Alternatively, the synthesis of **DB-H$_n$**·nPF$_6$ could also be performed (Fig. 3) by treating 3,5-dimethoxybenzylamine (**6**) and the diformyl-terminated oligomers **DA-*m*** (m = 0, 1, 2, 4, and 8) and employing synthetic protocols similar to those described earlier in this paragraph.

The mono- and diformyl-terminated oligomers, **MA-*m*** and **DA-*m***, respectively, are key intermediates in the synthesis of the dumbbell templates. Both compounds were prepared by efficient repetitive protocols. The syntheses of **MA-*m*** started with condensation between the commercially available 3,5-dimethoxybenzaldehyde (**MA-0**) and methyl 4-(aminomethyl)benzoate (**8a**), affording the expected imine, which was then converted (Fig. 4) into the free amine **9(0,0)** on treatment with $NaBH_4$. The amino group was protected with Boc groups by reacting the product with Boc_2O and triethylamine in $CHCl_3$ to yield the fully protected compound **10(0,0)**. The ester group in **10(0,0)** was then converted into a hydroxymethyl group in **11(0,0)** by reduction with lithium aluminum hydride in THF. Finally, the hydroxymethyl group was converted into a formyl function (compound **MA-1**) by oxidation of **11(0,0)** with pyridinium chlorochromate (PCC) in CH_2Cl_2. The aldehyde **MA-1** has a molecular structure similar to that of the aldehyde **MA-0**, except that it possesses an additional –$CH_2N(Boc)CH_2$– unit. Thus, by repeating this iterative synthetic cycle, the monoformyl-terminated compound **MA-2** was obtained after a four-step procedure.

Although this repetitive synthetic approach is straightforward and can lead conceptually to higher oligomers with $m > 3$, the growth of the repeating units is too tedious, requiring, as it does, multiple-step synthesis. To expedite the synthesis of the higher oligomers, that is, **MA-*m*** ($m > 2$), a compound analogous to **8a**,

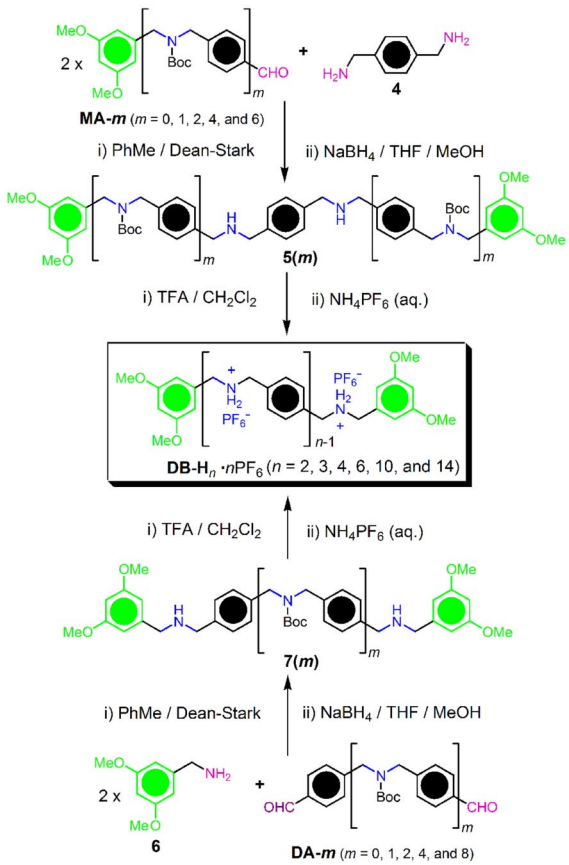

Fig. 3. Synthetic route to the dumbbell templates **DB-H$_n$**·nPF$_6$.

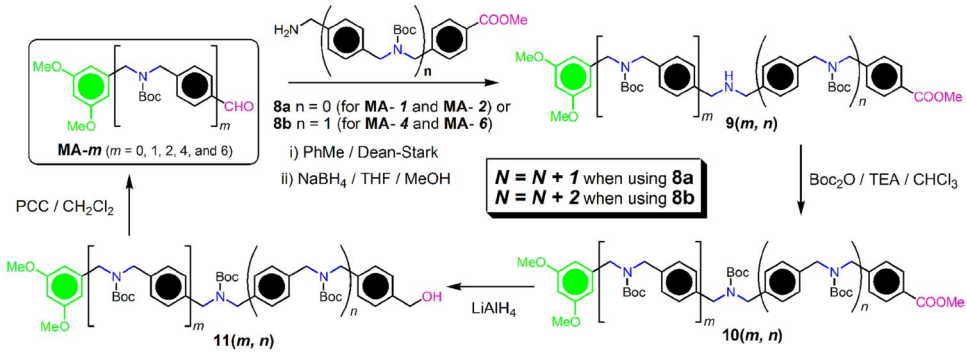

Fig. 4. Synthetic route to the monoformyl-terminated oligomers **MA-*m***.

namely **8b**, which carries an additional –$CH_2N(Boc)CH_2$– unit, was synthesized [see supporting information (SI) Scheme 3] and then used as another key building block in the subsequent synthetic work. By using the already established synthetic protocol, the formyl oligomers **MA-4** and **MA-6** were prepared in four and eight steps, respectively, from the aldehyde **MA-2** by involving the iterative synthesis cycles with **8b** as the building block in place of **8a**. Similarly, the bisformyl derivatives **DA-*m*** (m = 2, 4, and 8) were prepared (Fig. 5) by the same iterative procedure. The syntheses started with terephthaldehyde (**DA-0**). The dialdehyde **DA-2** was prepared by using **8a** as a building block. After each synthetic cycle, the number of N(Boc) units increases by 2 and 4, respectively. With all these intermediates to hand, dumbbells **DB-H$_n$**·$n$$PF_6$ (with n = 2, 3, 4, 6, 10, and 14) were produced in amounts in excess of 100 mg. All of these intermediates, as well as the final target compounds, were characterized by standard spectroscopic techniques (see *SI Text*). For example, the high-resolution electrospray ionization mass spectra (HR-ESI-MS) of the dumbbells **DB-H$_n$**·$n$$PF_6$, after neutralization with base, showed (SI Fig. 9) well defined isotopic distribution patterns for the $[M + H]^+$ molecular mass peaks. At the same time, they exhibit symmetrical-looking ^{1}H NMR spectra in agreement with the assigned molecular structures.

The clipping reactions to form the dynamic [n]rotaxanes were conducted in nitromethane ($MeNO_2$) by mixing together the dumbbell template **DB-H$_n$**·$n$$PF_6$ with n eq each of compounds **2a** and **3**. The condensations were followed by ^{1}H NMR spectroscopy and HR-ESI-MS analyses. The dumbbell templates **DB-H$_n$**·$n$$PF_6$ (especially in the higher oligomers) exhibited poor solubilities in $MeNO_2$, forming suspensions. Upon addition of **2a** and **3**, the mixtures turned into a clear, golden-yellow solution in a few minutes when the dumbbell templates **DB-H$_n$**·$n$$PF_6$ (where n = 2, 3, 4, and 6) were used, affording [3]-, [4]-, [5]-, and [7]rotaxanes, respectively. The ^{1}H NMR spectra demonstrated (Fig. 6) the complete formation of the corresponding [n + 1]rotaxanes. The distinct, sharp peaks that correlate with the [24]crown-8 macrocycle are observed; for example, the peaks for imine protons (*H*—C═N), the peaks for pyridine rings (a and b) and aryl rings (c–f), and ethylene glycol chains (not shown), are all in agreement with the peaks of the dynamic [2]rotaxane investigated in ref. 46. Interestingly, two sets of resonances are observed for the aromatic protons of the macrocycles present in the [4]-, [5]-, and [7]rotaxanes, the ratios between the two sets of signals calculated by integration of the spectra, being 2:1, 1:1, and 1:2, respectively. These observations can be explained by the constitutionally heterotopic environments of the macrocycles surrounding the dumbbells, that is, in the [4]rotaxane, the two homotopic macrocycles adjacent to the stopper (R_A, signals a–f) are heterotopic with respect to the central macrocycle (R_B, signals a′–f′). In the [5]rotaxane, rings R_A are different from rings R_B, and in [7]rotaxane, rings R_B and R_C share very similar chemical environments that differ from rings R_A. The slight difference between rings R_B and R_C is even expressed in the separation of the peaks for the imine protons (*H′*—C═N; Fig. 6*D*). In addition, the secondary dialkylammonium sites (–NH_2^+–) on the dumbbells also show two sets of signals for the higher [n]rotaxanes. The formation of these [n]rotaxanes is further supported (see SI Fig. 10) by their HR-ESI-MS. Intense peaks associated with the corresponding ions after the loss of a certain numbers of PF_6^- counterions are clearly observed in the mass spectra. All of these MS and ^{1}H NMR spectroscopic data prove that the template-directed, thermodynamic clipping approach already used in the preparation (46, 47) of the [2]rotaxane is also applicable for the higher-order [n]rotaxanes, at least as far as n = 7.

The formation of the [11]rotaxane (a 21-component self-assembly) and the [15]rotaxane (a 29-component self-assembly) using similar clipping protocols, however, encountered practical problems associated, most likely, with the extremely poor solubilities of the dumbbell templates in $MeNO_2$, conferring low solubilities on the rotaxanes as well. Specifically, the clipping reaction for

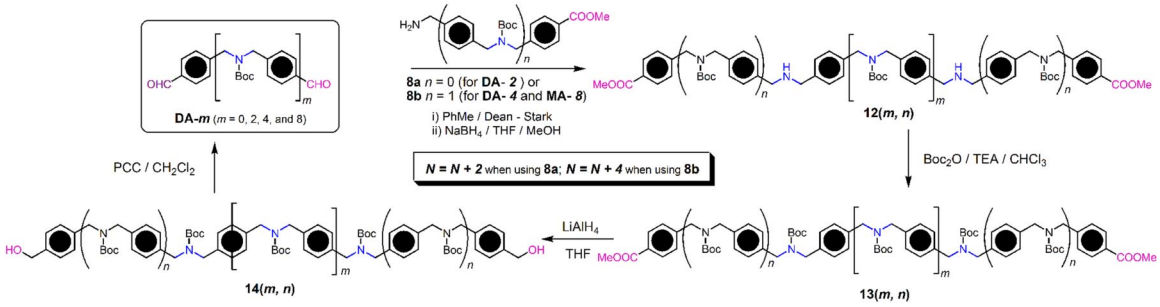

Fig. 5. Synthetic route to the bisformyl-terminated oligomers **DA-*m***.

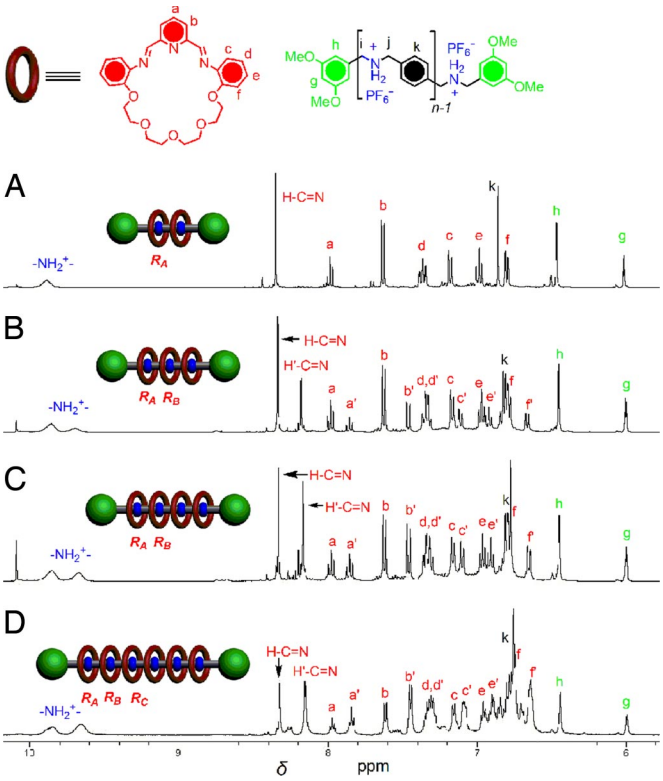

Fig. 6. Partial ^{1}H NMR spectra (400 MHz) of the dynamic [*n*]rotaxanes (n = 3, 4, 5, and 7) after mixing the corresponding dumbbells **DB-H$_n$**·nPF$_6$, **2a**, and **3** in CD_3NO_2 (δ = 5.8–10.2 ppm). Signals labeled with a–f are correlated to the resonances of the ring close to the stoppers (R_A), and the signals labeled with a′–f′ are assigned to the resonances of other rings (R_B and R_C). The peaks for protons i and j locate at about δ = 4.68 ppm (not shown).

the formation of the [11]rotaxane was performed under moderately dilute conditions, for example, 2.5 mg of the dumbbell in 10 ml of CD_3NO_2, wherein the mixture became nearly clear within 2 h. ^{1}H NMR spectra and HR-ESI-MS (not shown) revealed partial formation of the desired [11]rotaxane with other products dominating the reaction mixture. Changing the solvent to CD_3CN did not enhance the formation of the desired [11]rotaxane. The situation surrounding the formation of the [15]rotaxane was even more discouraging insofar as the suspension in the reaction did not become clear even under highly dilute conditions and with stirring at room temperature for several days. Heating of the reaction mixture led to decomposition of the starting materials.

To address these issues, we decided to use alkyloxyl pyridinedicarboxaldehyde **2b** (see SI Scheme 4 for its preparation) in which the additional octyloxyl unit is expected to improve significantly the solubilities of the polyrotaxanes formed. The clipping reactions of the dumbbells **DB-H$_n$**·nPF$_6$ with **2b** and **3** were conducted under conditions similar to those used with **2a** clipping reactions and work well in the formation of [*n*]rotaxanes (where n = 3, 4, 5, and 7), as indicated by the ^{1}H NMR spectroscopy and the HR-ESI-MS (see SI Figs. 11 and 12). Benefiting from the solubilizing groups present in **2b**, the clipping reaction of the dumbbell **DB-H$_{10}$**·10PF$_6$ with **2b** and **3** proceeds as rapidly as for the smaller [*n*]rotaxanes (where n = 3, 4, 5, and 7). A golden-yellow solution was obtained within a few minutes after mixing the components and the ^{1}H NMR spectrum shows (Fig. 7) clearly that the major species present in the CD_3NO_2 solution is the desired [11]rotaxane. It is similar to that of the [7]rotaxane prepared under similar conditions. Two sets of imine signals are observed for all the [*n*]rotaxanes when $n > 3$. The ratios calculated (Fig. 7*B*) from the peaks for the imine protons, *H*—C═N to *H*′—C═N is 1:4, confirm the efficient formation of the [11]rotaxane in which heterotopic rings R_B, R_C, R_D, and R_E have similar chemical environments and are markedly different from those of the rings R_A. The HR-ESI-MS of the mixture reveals intense peaks associated with the molecular ions $[M - 8PF_6]^{8+}$, $[M - 7PF_6]^{7+}$, $[M - 6PF_6]^{6+}$, $[M - 5PF_6]^{5+}$, and $[M - 4PF_6]^{4+}$ in the reliable mass/charge range (500–2,500) of the instrument (see SI Fig. 12*e*), once again supporting the formation of the [11]rotaxane.

Alas, however, mixing of the dumbbell **DB-H$_{14}$**·14PF$_6$ with **2b** and **3** in $MeNO_2$ failed to give a clear solution; even under highly dilute conditions and after prolonged stirring time, no convincing experimental data were obtained that pointed to the formation of the desired [15]rotaxane. The very low solubility of the dumbbell template finally put a limit on the template-directed, thermodynamic synthesis of the linear polyrotaxanes in one-pot reactions, at least with hexafluorophosphate anions as the counterions.

The dynamic [2]rotaxanes (see refs. 46 and 47) and some of the branched [4]rotaxane dendrimers (see refs. 48 and 49) containing imine bonds were "fixed" in their kinetically stable forms by reduction of the imine bonds with the BH_3·THF complex without any need for chromatographic separations. The reduction of the [*n*]rotaxanes (n = 3, 4, 5, 7, and 10) reported here is not such an easy task because all of the $(2n - 2)$ imine bonds in the macrocycles arranged along the dumbbell template have to be reduced at the same time. The dynamic [*n*]rotaxanes in $MeNO_2$ were reduced by addition of 1 M BH_3·THF complex (2 eq per imine bond). This solution was stirred at room temperature for 16 h. After removal of the solvent, the residue was treated with 2 M NaOH (aq) and extracted with $CHCl_3$ to give the neutral [*n*]rotaxanes. After purification by preparative TLC, the neutral [*n*]rotaxanes were acidified with TFA, and counterion exchange with saturated NH_4PF_6 (aq) afforded the fixed [*n*]rotaxanes. However, the efficiency of the fixing process has its limitations with the increasing numbers of macrocycles. The pure fixed [3]-, [4]-, and [5]rotaxanes were isolated in 77%, 74%, and 40% yields, respectively. All of these [*n*]rotaxanes were purified by preparative TLC to remove impurities remaining after reduction. The reduction of dynamic [7]rotax-

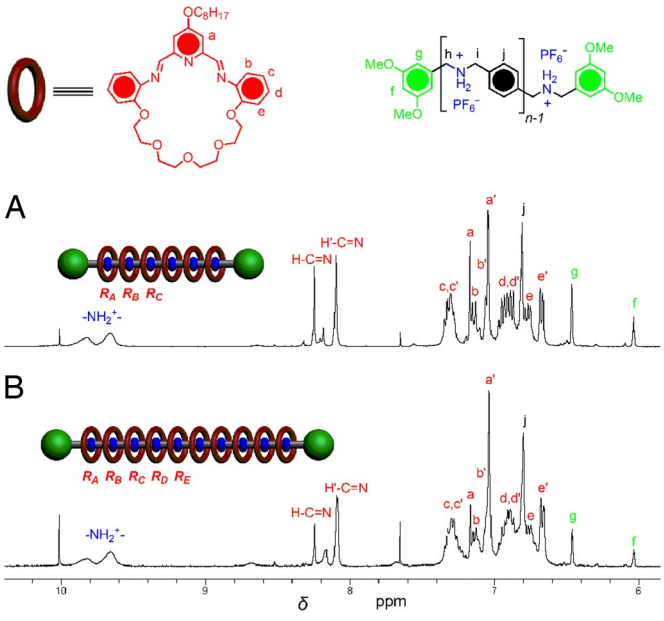

Fig. 7. Partial ^{1}H NMR spectra (400 MHz) of the dynamic [*n*]rotaxanes (n = 7 and 11) after mixing the corresponding dumbbells **DB-H$_n$**, **2b**, and **3** in CD_3NO_2 (δ = 5.8–10.4 ppm). Signals labeled with a–e are correlated with the resonances of the rings close to the stoppers (R_A), and the signals labeled with a′–e′ are assigned to the resonances of other rings (R_B, R_C, R_D, and R_E). The peaks for protons i and j locate at about δ = 4.69 ppm (not shown).

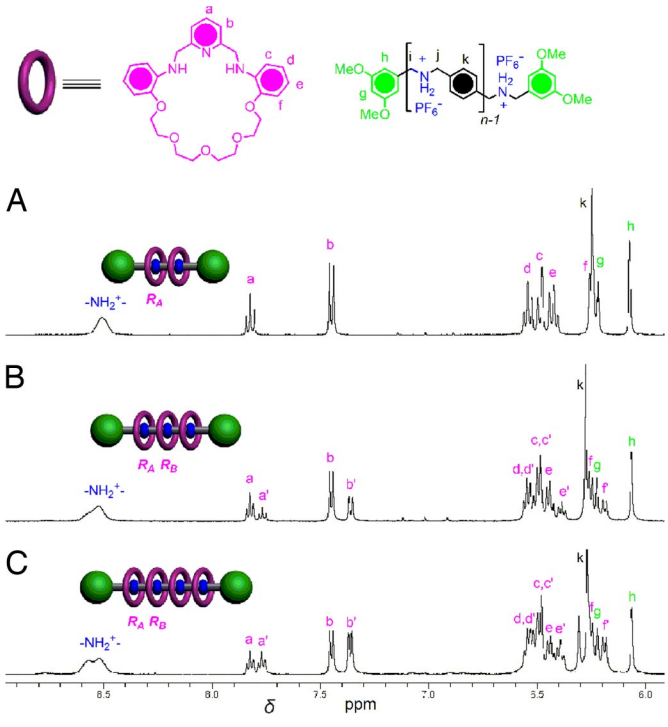

Fig. 8. Partial ^{1}H NMR spectra (400 MHz) of the fixed [*n*]rotaxanes (*n* = 3, 4, and 5) in CD_3SOCD_3 (δ = 5.8–9.0 ppm). Signals labeled with a–f are correlated with the resonances of the rings close to the stoppers (R_A), and the signals labeled with a′–f′ are assigned to the resonances of other rings R_B. The peaks for protons i and j locate at about δ = 4.75 ppm (not shown).

ane and [11]rotaxane yielded large amounts of by-products from which the fully fixed rotaxanes could not be separated. This limitation is ascribed to the partial cleavage and dissociation of the macrocycles from the dumbbell templates during the reduction. This observation is comparable to the fixing process in the higher-order branched [4]rotaxane dynamic dendrimers, where steric hindrance is also operative (49). The diffusion of the BH_3·THF to the imine bonds and the subsequent reduction has to compete with the imine dissociation process, and this balance is more difficult to control with the higher-order [*n*]rotaxanes. The ^{1}H NMR spectra of the pure [3]-, [4]-, and [5]rotaxanes are shown in Fig. 8. The [4]- and [5]rotaxanes display two sets of resonance signals for the fixed macrocycles, with the integration ratios of 2:1 and 1:1, respectively. This observation, again, can be explained by the environments of rings R_A compared with rings R_B. Similarly, two sets of resonance signals for the $-NH_2^+-$ protons can also be observed. The structural assignments of the [3]-, [4]-, and [5]rotaxanes are further supported (SI Fig. 13) by the HR-ESI-MS, wherein intense peaks correspond to positive ions after the loss of a certain number of PF_6^- ions. All the peaks give isotopic distributions in agreement with the calculated values.

Conclusion

We have developed a highly efficient template-directed, thermodynamically controlled clipping approach to some well defined, homogeneous [*n*]rotaxanes (with *n* to 11). The synthesis is based on the formation of two imine bonds in a [24]crown-8 macrocycle from acyclic precursors, a dialdehyde and a diamine, by dynamic covalent chemistry in the presence of secondary dialkylammonium ion templates present in specifically synthesized and well characterized dumbbells. Because this protocol represents one of the most efficient ways to make mechanically interlocked compounds, one might expect that it will also be applied to the template-directed synthesis of even more intricate compounds, including molecular necklaces, dendritic polyrotaxanes, polycatenanes, and so on. Although the extent of [*n*]rotaxane formation is so far limited to *n* = 11 (a 21-component self-assembly process) because of solubility constraints, they could be overcome in the future by attaching solubilizing groups to the dumbbell templates as well as to macrocycles. The efficiency of the fixing of dynamic [*n*]rotaxanes by reduction of the imine bonds shows some dependence on *n*, that is, it occurs with decreased efficiency as *n* becomes larger. The fixed [3]-, [4]-, and [5]rotaxanes as pure, well characterized compounds have been successfully prepared.

The importance of being able to synthesize, in high yields, [*n*]rotaxanes, where *n* is a double-digit number, cannot be overly stressed. (While this manuscript was being written, Leigh's group described an alternative approach to the synthesis of [*n*]rotaxanes by using a template-directed clipping methodology. The distinctiveness of their approach lies in the controlled iterative addition of macrocycles onto a *single* binding site on the rotaxanes' dumbbell precursor. See ref. 50.) Such polyrotaxanes, in particular, when both the dumbbell and ring component can carry (positive) charges and so give the mechanically interlocked polyelectrolyte character, are candidates for studying the dependence of their rheological behavior on pH, on the choice of anions and solvents, and so forth. Also, [*n*]rotaxanes into which constitutionally different rings have been inserted in a controlled manner hold promise as templates for the production of artificial main-chain polymers containing numerous monomer units whose sequence can be predetermined in a manner reminiscent of many biopolymers.

Materials and Methods

Compound **3** was synthesized according to the procedure reported in ref. 46. All of the other starting materials are commercially available from Aldrich (St. Louis, MO) or VWR (West Chester, PA) and were used as received. All solvents were purified and dried before use. Column chromatography was performed on Silica Gel 60 (Merck, Whitehouse Station, NJ; 40–60 μm, 230–400 mesh). Deuterated solvents (Cambridge Isotope Laboratories, Cambridge, MA) for NMR spectroscopic analysis were used as received. All NMR spectra were recorded on Avance-400 (Bruker, Billerica, MA; at 400 MHz) and Avance-500 (Bruker; at 500 MHz) spectrometers. All chemical shifts are quoted in parts per million relative to tetramethylsilane with the residual solvent peak as a reference standard. Mass spectra were recorded on an Ion Spec 7·OT Ultima FTMS with ESI or MALDI-TOF ion sources. Detailed synthetic procedures and spectroscopic characterizations of all of the new intermediate compounds and the desired dumbbells (**DB-H**$_n$·*n*PF_6) are presented in the *SI Text*. The template-directed thermodynamic clipping reactions and subsequent fixing reactions were performed by using a general protocol summarized as follows.

The dumbbell template, **DB-H**$_n$·*n*PF_6 (5–10 mg), compound **2a** or **2b** (*n* eq), and compound **3** (*n* eq) were mixed in a minimum amount of CD_3NO_2 (0.75–2 ml). A clear golden-yellow solution was obtained in a few minutes (for *n* = 10 using **2b**). ^{1}H NMR spectra and ESI mass spectra of the solution were recorded until they did not register any changes over a 24-h period. A 1 M BH_3·THF complex in THF (2 eq per imine bond) was added to the solution. The reduction was complete in 16 h as observed by ^{1}H NMR spectroscopy. The solvents were removed under vacuum, and 2 M NaOH (aq) and $CHCl_3$ were added. The organic layer was washed with H_2O and dried (Na_2SO_4), and the solvent was removed under vacuum. The residue was then purified by preparative TLC on silica gel plates by using different eluents ($CHCl_3$/MeOH = 4:1 for the [3]rotaxane; $CHCl_3$/Et_3N = 3:2 for the [4]- and [5]rotaxanes) to give the neutral rotaxanes, which were dissolved in CH_2Cl_2 before a few drops of TFA were added. The solvents were then removed under vacuum, and the residue was redissolved in a minimum amount of MeOH. Saturated aqueous NH_4PF_6 was next added to the solution to yield a white precipitate. The mixture was concentrated under

vacuum to remove the excess of MeOH and the precipitate was collected, washed with H_2O, and dried under vacuum in the presence of P_2O_5. Pure, fixed [3]-, [4]-, and [5]rotaxanes were isolated in 77%, 74%, and 40% yields, respectively. The fixed higher-order [*n*]rotaxanes could not be isolated.

We thank the following organizations for their generous financial support: the National Science Foundation, the Microelectronics Advanced Research Corporation, its focus center on Functional Engineered NanoArchitectonics, the Defense Advanced Research Projects Agency, and the Center for Nanoscale Innovation for Defense.

1. Anelli PL, Spencer N, Stoddart JF (1991) *J Am Chem Soc* 113:5131–5133.
2. Bissell RA, Cordova E, Kaifer AE, Stoddart JF (1994) *Nature* 369:133–137.
3. Andersson M, Linke M, Chambron JC, Davidson J, Heitz V, Hammarstrom L, Sauvage JP (2002) *J Am Chem Soc* 124:4347–4362.
4. Asakawa M, Brancato G, Fanti M, Leigh DA, Shimizu T, Slawin AMZ, Wong JKY, Zerbetto F, Zhang S (2002) *J Am Chem Soc* 124:2939–2950.
5. Iijima T, Vignon SA, Tseng HR, Jarrosson T, Sanders JKM, Marchioni F, Venturi M, Apostoli E, Balzani V, Stoddart JF (2004) *Chem Eur J* 10:6375–6392.
6. Dietrich-Buchecker CO, Sauvage JP, Kern JM (1984) *J Am Chem Soc* 106:3043–3045.
7. Ashton R, Goodnow TT, Kaifer AE, Reddington MV, Slawin AMZ, Spencer N, Stoddart JF, Vicent C, Williams DJ (1989) *Angew Chem Int Ed Engl* 28:1396–1399.
8. Kidd TJ, Leigh DA, Wilson AJ (1999) *J Am Chem Soc* 121:1599–1600.
9. Bäuerle P, Ammann M, Wilde M, Götz G, Steritz EMO, Rang A, Schalley CA (2007) *Angew Chem Int Ed* 46:363–368.
10. Blight BA, Wisner JA, Jennings MC (2007) *Angew Chem Int Ed* 46:2835–2838.
11. Williams AR, Northrop BH, Chang T, Stoddart JF, White AJP, Williams DJ (2006) *Angew Chem Int Ed* 45:6665–6669.
12. Northrop BH, Spruell JM, Stoddart JF (2007) *Chem Today* 25(3):4–7.
13. Dietrich-Buchecker C, Rapenne G, Sauvage JP (1997) *Chem Commun* 2053–2054.
14. Ashton PR, Matthews OA, Menzer S, Raymo FM, Spencer N, Stoddart JF, Williams DJ (1997) *Liebigs Ann Chem* 2485–2494.
15. Adams H, Ashworth E, Breault GA, Guo J, Hunter CA, Mayers PC (2001) *Nature* 411:763.
16. Brüggemann J, Bitter S, Müller S, Müller WM, Müller U, Maier NM, Lindner W, Vögtle F (2006) *Angew Chem Int Ed* 46:254–259.
17. Kelley RF, Tauber MJ, Wasielewski MR (2006) *Angew Chem Int Ed* 45:7979–7982.
18. Chichak KS, Cantrill SJ, Pease AR, Chiu SH, Cave GWV, Atwood JL, Stoddart JF (2004) *Science* 304:1308–1312.
19. Pentecost CD, Chichak KS, Peters AJ, Cave GWV, Cantrill SJ, Stoddart JF (2006) *Angew Chem Int Ed* 46:218–222.
20. Pentecost CD, Tangshaivang N, Cantrill SJ, Chichak KS, Peters AJ, Stoddart JF (2007) *J Chem Educ* 84:855–859.
21. Pentecost CD, Chichak KS, Peters AJ, Cave GWV, Cantrill SJ, J Stoddart F (2007) *Angew Chem Int Ed* 46:218–222.
22. Stoddart JF, Tseng HR (2002) *Proc Natl Acad Sci USA* 99:4797–4800.
23. Collier CP, Mattersteig G, Wong EW, Luo Y, Beverly K, Sampaio J, Raymo FM, Stoddart JF, Heath JR (2000) *Science* 289:1172–1175.
24. Green JE, Choi JW, Boukai A, Bunimovich Y, Johnston-Halperin E, DeIonno E, Luo Y, Sheriff BA, Xu K, Shin YS, *et al.* (2007) *Nature* 445:414–417.
25. Liu Y, Flood AH, Bonvallet PA, Vignon SA, Northrop BH, Tseng HR, Jeppesen JO, Huang TJ, Brough B, Baller M, *et al.* (2005) *J Am Chem Soc* 127:9745–9759.
26. Berná J, Leigh DA, Lubomska M, Mendoza SM, Pérez EM, Rudolf P, Teobaldi G, Zerbetto F (2005) *Nat Mater* 4:704–710.
27. Nguyen TD, Tseng HR, Celestre PC, Flood AH, Liu Y, Stoddart JF, Zink JI (2005) *Proc Natl Acad Sci USA* 102:10029–10034.
28. Nguyen TD, Liu Y, Saha S, Leung KCF, Stoddart JF, Zink JI (2007) *J Am Chem Soc* 129:626–634.
29. Saha S, Leung KCF, Nguyen TD, Stoddart JF, Zink JI (2007) *Adv Funct Mater* 17:685–693.
30. Harada A, Li J, Kamachi M (1992) *Nature* 356:325–327.
31. Gong CG, Ji Q, Subramaniam C, Gibson HW (1998) *Macromolecules* 31:1814–1818.
32. Raymo FM, Stoddart JF (1999) *Chem Rev* 99:1643–1663.
33. Aricó F, Badjić JD, Cantrill SJ, Flood AH, Leung KCF, Liu Y, Stoddart JF (2003) *Top Curr Chem* 249:203–259.
34. Bravo JA, Raymo FM, Stoddart JF, White AJP, Williams DJ (1998) *Eur J Org Chem* 2565–2571.
35. Seel C, Vögtle F (2000) *Chem Eur J* 6:21–24.
36. Fuller AM, Leigh DA, Lusby PJ, Oswald IDH, Parsons S, Walker DB (2004) *Angew Chem Int Ed* 43:3914–3918.
37. Brady PA, Sanders JKM (1997) *Chem Soc Rev* 26:327–336.
38. Rowan SJ, Cantrill SJ, Graham RL, Cousins RL, Sanders JKM, Stoddart JF (2002) *Angew Chem Int Ed* 41:898–952.
39. Mobian P, Kern JM, Sauvage JP (2004) *Angew Chem Int Ed* 43:2392–2395.
40. Badjić JD, Cantrill SJ, Grubbs RH, Guidry EN, Orenes R, Stoddart JF (2004) *Angew Chem Int Ed* 43:3273–3278.
41. Layer WR (1963) *Chem Rev* 63:489–510.
42. Huc I, Lehn JM (1997) *Proc Natl Acad Sci USA* 94:2106–2110.
43. Kubota Y, Sakamoto SS, Yamaguchi K, Fujita M (2002) *Proc Natl Acad Sci USA* 99:4854–4856.
44. Wang L, Myroslav OV, Bogdan A, Bolte M, Böhmer V (2004) *Science* 304:1312–1214.
45. Guidry EN, Cantrill SJ, Stoddart JF, Grubbs RH (2005) *Org Lett* 7:2129–2132.
46. Glink PT, Oliva AI, Stoddart JF, White AJP, Williams DJ (2001) *Angew Chem Int Ed* 40:1870–1875.
47. Aricó F, Chang T, Cantrill SJ, Khan SI, Stoddart JF (2005) *Chem Eur J* 11:4655–4666.
48. Leung KCF, Aricó F, Cantrill SJ, Stoddart JF (2005) *J Am Chem Soc* 127:5808–5810.
49. Leung KCF, Aricó F, Cantrill SJ, Stoddart JF (2007) *Macromolecules* 40:3951–3959.
50. Fuller AML, Leigh DA, Lusby PJ (2007) *Angew Chem Int Ed* 46:5015–5019.